Copyright Protection by Watermarking for Color Images against Rotation and Scaling Attacks Using Peak Detection and Synchronization in Discrete Fourier Transform Domain*

Yen-Chung Chiu and Wen-Hsiang Tsai

Department of Computer and Information Science
National Chiao Tung University
Hsinchu, Taiwan 300

gis91528@cis.nctu.edu.tw

whtsai@cis.nctu.edu.tw

ABSTRACT

A watermarking method for copyright protection of color images against rotation and scaling attacks is proposed. A watermark is embedded in an input image as coefficient-value peaks circularly and symmetrically distributed in a middle band of the discrete Fourier transform (DFT) domain of the input image. By detecting the peaks in the DFT domain of the resulting stego-image, the embedded watermark can be extracted for copyright proof, even after the stego-image is attacked by rotation and rescaling. Experimental results showing the effectiveness of the proposed method are also included.

Keywords: watermarking, copyright protection, color image, rotation, scaling, discrete Fourier transform, coefficient-value peaks, synchronization peak.

1. INTRODUCTION

Digital watermarking is a technique for embedding a watermark into a digital image to protect the owner's copyright of the image. The embedded watermark in the resulting stego-image must be robust because the stego-image may be rotated or scaled by illicit users. It is desirable that after such *rotation or scaling attacks*, the watermark is not fully destroyed and can still be extracted to verify the copyright of the image.

Many watermarking techniques for copyright protection have been proposed in recent years. Watermarking techniques that are robust against rotation and scaling are mostly performed in the frequency domain. O'Ruanaidh and Pun [1] proposed the use of Fourier-Mellin transform-based invariants for digital image watermarking. A public watermarking method based on the Fourier-Mellin transform and an extension of it based on the Radon transform was proposed by Wu, et al. [2]. In Lin, et al. [3], a watermark was embedded into a one-dimensional signal obtained by taking the Fourier transform of the image, re-sampling the Fourier magnitudes into log-polar coordinates, and summing a function of those magnitudes along the log-radius axis. Su and Kuo [4] proposed a spatial-frequency composite digital image watermarking scheme to make the embedded watermark survive rotation and scaling attacks. The frequency-domain watermark was embedded in the discrete Fourier transform (DFT) coefficients. The spatial-domain watermarking

* This work was supported partially by the NSC 92-2422-H009-010

is used to help recover the image to its original orientation and scale.

In this paper, we propose a watermarking method for copyright protection of color images against rotation and scaling attacks by the use of coefficient-value peaks in the DFT domain. A watermark in the form of a binary stream is embedded as coefficient-value peaks distributed circularly and symmetrically in a middle band of the DFT coefficients of an input image. By detecting and synchronizing the coefficient-value peaks of the resulting stego-image, the embedded watermark can be extracted, even after the stego-image is subjected to rotation and rescaling attacks. Experimental results show the effectiveness of the proposed method.

The remainder of this paper is organized as follows. In Section 2, the idea of the proposed method will be described. In Section 3, the proposed watermark embedding process will be presented. In Section 4, the proposed watermark extraction process will be described. In Section 5, some experimental results will be illustrated. Finally, in Section 6 a summary will be made.

2. Idea of Proposed Method

2.1 Properties of DFT and Color Images

The DFT $F(u, v)$ of an input image $f(x, y)$ of size $M \times N$ can be described by:

$$F(u,v) = \frac{1}{MN}\sum_{x=0}^{M-1}\sum_{y=0}^{N-1} f(x,y)e^{-j2p(ux/M+vy/N)}. \quad (1)$$

This transform has several properties related for this study. First, the transform has a symmetry property [5] shown by

$$F(u, v) = F^*(-u, -v), \quad (2)$$

where the symbol F^* means the complex conjugate of F. Also, the complex transform $F(u, v)$ can be divided into two parts, the *magnitude function* (or called *spectrum*) $|F(u, v)| = [R^2(u, v) + I^2(u, v)]^{1/2}$ and the *phase function* $f(u, v) = \tan^{-1}[I(u, v)/R(u, v)]$, where $R(u, v)$ and $I(u, v)$ are the real and imaginary parts of $F(u, v)$, respectively. For real inputs like images, Eq. (2) leads to:

$$|F(u, v)| = |F(-u, -v)|, \quad (3)$$

which means that a coefficient value and its symmetric version in the DFT domain are equal in magnitude. In addition, both the magnitude and the phase functions are necessary for complete reconstruction of an input image from its DFT. But the magnitude part is less important than the phase part. The magnitude-only image is unrecognizable. On the contrary, the phase-only image is barely recognizable [6]. Therefore, we may compute and adjust the magnitudes of the DFT coefficients to embed information without causing significant loss of the image quality, as is done in this study.

Furthermore, it is well known [7] that the rescaling operation has almost no effect on the DFT coefficients, and that after rotating an image in the spatial domain, the locations of the coefficient values, on the contrary, will have the same rotation in the DFT domain. Figs. 1(a) and (b) show an image and a rotated version of it. And the corresponding *spectrum images*, in which each pixel value is taken to be the magnitude of a DFT coefficient, are shown in Figs. 1(c) and (d), respectively. Note that the spectrum image in Fig. 1(d) has the same rotation as the image in Fig. 1(b).

Finally, though we can embed watermark information into all the three color channels of an image in general, according to experiments, this work can only be conducted in the red and blue channels in the DFT domain because hiding information in the green channel is too sensitive to the human vision and will create perceivable effects.

2.2 Proposed Technique of Using DFT Peaks for Watermarking

In the proposed watermarking method, after the zero frequency point $F(0,0)$ is shifted to the center of the DFT domain, a watermark is embedded in a ring region which covers a middle band, denoted as B subsequently, in the frequency domain between two circles with two pre-selected radii R_1 and R_2 where

$R_1 < R_2$, as shown in Fig. 2. The middle band of the frequency domain is divided into n equally-spaced concentric circles with radii $r_1, r_2, \cdots, r_n$, and into m angle ranges with starting angles $q_1, q_2, \cdots, q_m$, as seen in Fig. 3. Then, $n\times m$ *embeddable positions* $p_1, p_2, \cdots, p_{n\times m}$ are selected in this study to be located at (u_k, v_k) in the frequency domain described by:

$$p_k = (u_k, v_k) = (r_i \cos q_j, r_i \sin q_j), \qquad (4)$$

where $1 \le i \le n$, $1 \le j \le m$ and $1 \le k \le n\times m$, and at each embeddable position p_k, the coefficient value is adjusted to be a *local peak* in the frequency domain.

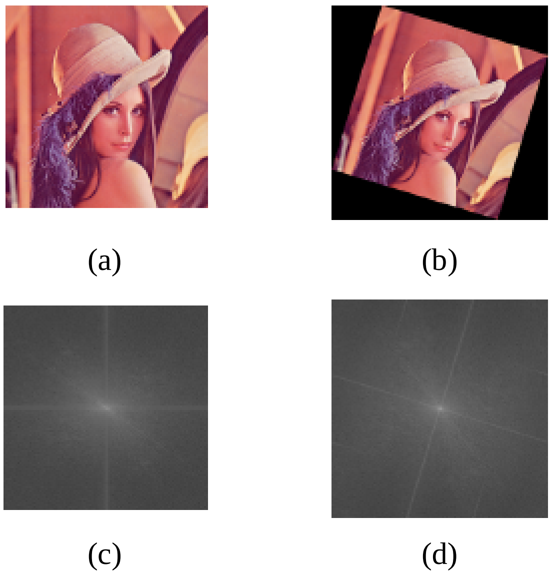

Fig. 1 Input images and Fourier spectrums of G channel. (a) Image "Lena". (b) Image "Lena" after rotation. (c) Fourier spectrum of "Lena" (d) Fourier spectrum with the same rotation of (b).

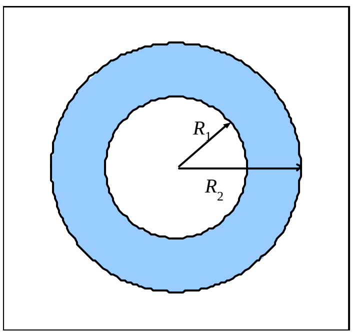

Fig. 2 A ring region in middle frequency band.

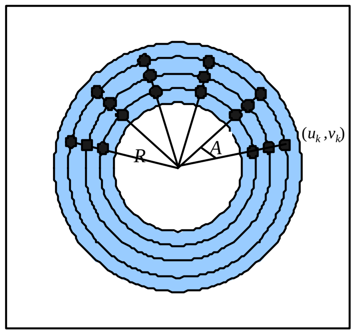

Fig. 3 The ring region divided into concentric circles and into angular sectors.

More specifically, let W be a watermark to be embedded, which is taken to be a serial number in this study in the form of a bit stream, and let $M(u_k, v_k)$ be the DFT coefficient value at an embeddable position $p_k = (u_k, v_k)$. Then, we embed a *watermark bit* w_i at p_k in the frequency domain in this study by modifying $M(u_k, v_k)$ to be *a local peak* $M'(u_k, v_k)$ by the following equation:

$$M'(u_k, v_k) = M(u_k, v_k) + c\times w_i \qquad (5)$$

where c is a pre-selected parameter that determines the strength of the embedded watermark signal.

It is noted that, when conducting watermarking in the above way of changing the DFT coefficient value at an embeddable position $p_k = (u_k, v_k)$ for the amount of $d = c\times w_i$, we must preserve the *positive symmetry* property of the DFT [9] by changing the corresponding coefficient value at $p_k' = (-u_k, -v_k)$ for the same amount d. Otherwise, the peak created at p_k will be counteracted by the symmetric coefficient value at p_k' after applying the inverse DFT. That is, we must perform, as is done in this study, the following operation

$$M'(-u_k, -v_k) = M(-u_k, -v_k) + d \qquad (6)$$

in addition to (5) each time we embed a watermark bit w_i at an embeddable position $p_k = (u_k, v_k)$.

2.3 Proposed Technique for Synchronizing Peak Locations for Protection against Rotation and Scaling Attacks

In order to deal with rotation and scaling attacks, an extra local peak P_{sync}, called *synchronization peak*, is created in the DFT domain to serve as a signal for *synchronizing* the peak locations p_1, p_2, …, $p_{n\times m}$ mentioned previously in a way described later. P_{sync} is embedded into the previously-mentioned middle frequency band B at a location p_{sync} described by:

$$
\begin{aligned}
p_{sync} &= (u_{sync}, v_{sync}) \\
&= (r_{sync}\cos q_{sync}, r_{sync}\sin q_{sync}) \qquad (7)
\end{aligned}
$$

where r_{sync} is selected to be larger than R_2 and q_{sync} is a pre-selected angle value. We adjust the DCT value M of P_{syn} to be a peak value $M' = M + c$ where c is the constant value mentioned previously.

We now describe how we use the synchronization peak P_{sync} in the proposed watermark extraction process to calculate the rotation angle of a tampered stego-image which suffered possibly from a rotation attack. Because of the DFT properties mentioned previously and illustrated by Fig. 1, if a stego-image is rotated, the location of P_{sync} will also be changed with the same rotation angle. We may calculate first the new angle q'_{sync} of P_{sync} and take the difference Δq between q'_{sync} and q_{sync} to decide whether the stego-image has been rotated: if $\Delta q \neq 0$, then rotated; else, not. If rotated, then we find the angles q'_k of the remaining local peaks, and compute their original angles q''_k by

$$q''_k = q'_k - \Delta q. \qquad (8)$$

On the other hand, as mentioned previously, if a stego-image is rescaled, the DFT coefficient values are almost unaffected. It means that the radii of the local peaks will not be changed.

3. Watermark Embedding Process

In the proposed watermark embedding process, we use the red and blue color channels of an input image to embed a watermark bit stream in the DFT domain according to the idea described in Section 2. Each channel is used to embed a half of the watermark bit stream. The inputs to the proposed watermark embedding process are a color image C and a watermark bit stream W. The output is a stego-image S. The process is described as an algorithm as follows.

Algorithm 1: *Watermark embedding process.*

Input: a color image C and a watermark bit stream $W = w_1w_2\cdots w_{2\ell}$ with length 2ℓ, where $\ell = m\times n$ with m and n being two pre-selected integer numbers.

Output: A stego-image S.

Steps.

1. Transform the red and blue channels of C into the frequency domain by the DFT to get C'_{red} and C'_{blue}.
2. Divide W into two parts $W_{\text{red}} = w_1w_2\cdots w_\ell$ and $W_{\text{blue}} = w_{\ell+1}w_{\ell+2}\cdots w_{2\ell}$.
3. Embed W_{red} and W_{blue} into C'_{red} and C'_{blue}, respectively, by performing the following operations.
   3.1 Decide ℓ embeddable positions $P = \{p_1, p_2, \cdots, p_\ell\}$ and their symmetric positions $Q = \{q_1, q_2, \cdots, q_\ell\}$ in the middle frequency band of the DFT domain according to the way described in Section 2.2.
   3.2 If watermark bit w_k equals 1, then adjust the pair of the coefficient values located at p_k and q_k to be local peaks by Eqs. (5) and (6), where $1 \le k \le \ell$ for C'_{red} or $\ell + 1 \le k \le 2\ell$ for C'_{blue}.
   3.3 Add a synchronization peak P_{sync} according to the scheme described in Section 2.3.
4. Transform both C'_{red} and C'_{blue} back into the spatial domain by the inverse DFT.
5. Take the final result as the desired stego-image S.

4. Watermark Embedding Process

In the proposed watermark extraction process, the red and blue channels of a stego-image are accessed. Each of these two channels is transformed into the DFT domain. Then, the local peaks in the middle frequency band of the DFT domain are detected using a pre-selected threshold value T: if any DFT coefficient value M is larger than T, it is judged to be a local peak. Because of the symmetry property of the DFT coefficient values, we may only detect peaks within the range of the upper-half Fourier spectrum image. After collecting all the peaks, a detected peak with the largest radius r_{sync} and angle q_{sync} is taken to be the synchronization peak, which is then used to synchronize all the remaining peaks in a way described by (8). The result is a set of local peaks $P' = \{p'_1, p'_2, \cdots, p'_h\}$.

Also, we divide the ring area of the middle frequency band B between the two circles with radii R_1 and R_2 into n equally-spaced concentric circles and into m angle ranges to make B become a set of ℓ sectors $D = \{d_1, d_2, \cdots, d_\ell\}$ where $\ell = m \times n$, as seen in Fig. 4. Then, we compare P' and D to decide the watermark bit stream $W = w_1 w_2 \cdots w_\ell$ by:

$$w_k = \begin{cases} 1 & \text{if certain } p_i' \text{ falls in } d_k, \\ 0 & \text{otherwise,} \end{cases} \tag{9}$$

where $1 \le k \le \ell$ and $1 \le i \le h$. This means that, if there is a peak within a sector d_k, the bit w_k is set to be "1;" otherwise, "0." Finally, we transform the bit stream into an integer number as the extracted watermark and complete the watermark extraction process. The detail of the process can be described as an algorithm as follows.

Algorithm 2: *Watermark extraction process.*
Input: a stego-image S.
Output: a watermark W.
Steps.

1. Transform the red and blue color channels of S into the DFT domain to get two Fourier spectra S'_{red} and S'_{blue}.
2. Detect peaks within the upper halves of S'_{red} and S'_{blue}, respectively, by performing the following operations.

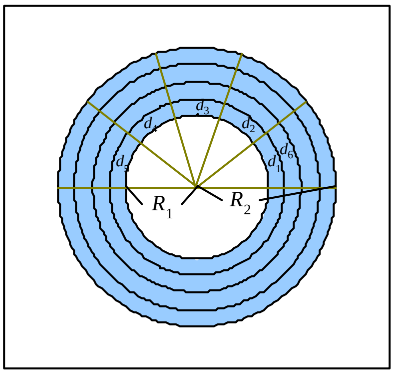

Fig. 4 The middle frequency band is divided into concentric sectors.

   2.1 Use a threshold value T to detect peaks in the middle-frequency band B mentioned previously. If the coefficient value at a location is larger than T, it is considered as a peak.
   2.2 Select the peak with the largest radius as the synchronization peak P_{sync}, and calculate its angle change Δq with respective to the original angle of the synchronization peak.
   2.3 Reconstruct the angles of the remaining peaks by Eq. (8) to get their new locations $P' = \{p'_1, p'_2, \cdots, p'_h\}$.
   2.4 Divide the middle frequency band B into ℓ sectors $D = \{d_1, d_2, \cdots, d_\ell\}$ where $\ell = n \times m$ as described in Algorithm 1.
   2.5 Compare P' and D to decide the watermark bit stream according to the way specified by Eq. (9).
3. Concatenate the two watermark bit streams obtained from processing S'_{red} and S'_{blue} sequentially, and transform the result into a serial number as the desired watermark W.

5. Experimental Results

Some experimental results of applying the proposed method are shown here. A serial-number watermark 877 was transformed into a bit stream. The factor c that determines the embedded watermark strength was assigned to be 1.5. Fig. 5

shows an input image with size 512×512. And Fig. 6(a) shows the stego-image of Fig. 5 after embedding the watermark. In addition, Figs. 6(b) and (c) show the corresponding Fourier spectrum image and the detected locations of the local and the synchronization peaks marked with red and green marks, respectively. Fig. 6(d) show a rotated version of Fig. 6(a) and the corresponding Fourier spectrum image and the detected peak locations are shown in Figs. 6(e) and (f), respectively. It shows that the Fourier spectrum image has the same angle of rotation as the tampered image. Fig. 7(a) shows a rescaled image of Fig. 6(a) and the corresponding Fourier spectrum image with the detected peaks is shown in Fig. 7(b). As can be seen, the embedded peaks can be successfully detected in our experiments.

Figs. 8(a) and (b) show two other color images both with size 512×512. And the corresponding stego-images after embedding the watermark are shown in Figs. 8(c) and (d), respectively. The corresponding PSNR values listed in Table 1 show that the quality of the stego-images is still good and that the embedded watermark is imperceptible by human vision.

6. Discussions and Summary

In this paper, we have proposed a method for embedding a watermark into a color image by coding and synchronization of coefficient-value peak locations in the DFT domain. Utilizing some properties of image coefficients in the DFT domain, we can embed a watermark in the form of a binary stream by creating the peaks circularly and symmetrically in a middle frequency band in the transform domain. On the other hand, an extra synchronization peak is added to synchronize the peak locations. The embedded watermark was shown by the experimental results to be robust against rotation and scaling attacks, thus achieving the goal of image copyright protection. However, the data hiding capability of the proposed watermark embedding method is not large and cannot accommodate a normal-sized logo image. It may be tried to solve this problem in the future.

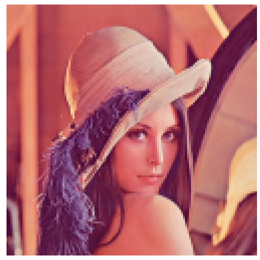

Fig. 5 An input image "Lena".

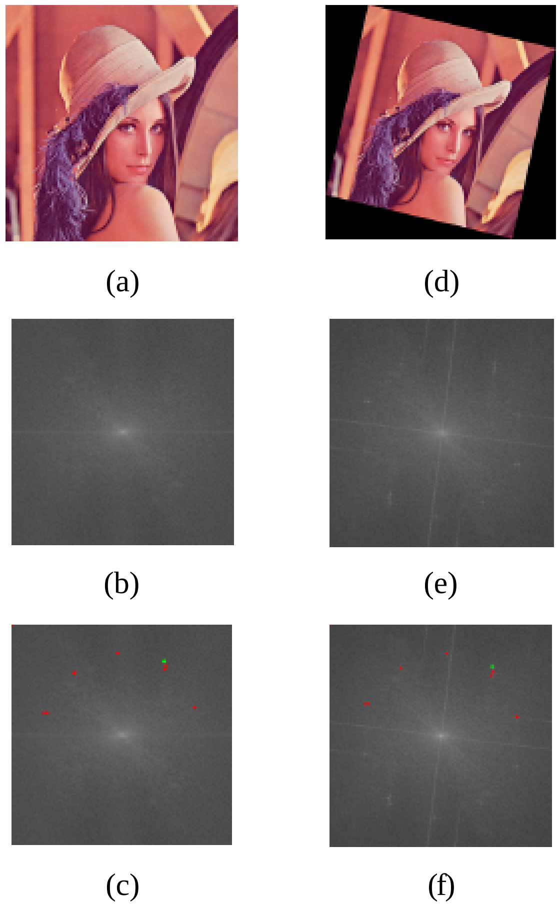

Fig. 6 Output stego-images with the watermark, the tampered image, and the Fourier spectrum images. (a) Stego-image "Lena". (b) Fourier spectrum image of (a). (c) Peak locations of (c). (d) Tampered image after rotating 13 degree clockwise. (e) Fourier spectrum image of (d). (f) Peak locations of (e).

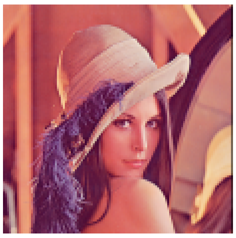

(a)

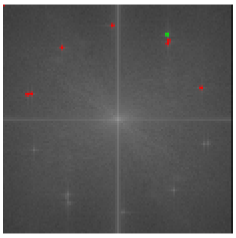

(b)

Fig. 7 A tampered image and its Fourier spectrum image. (a) Tampered image after rescaling to 90%. (b) Fourier spectrum image of (a) with peak locations.

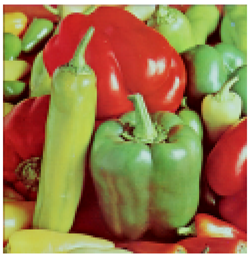

(a)

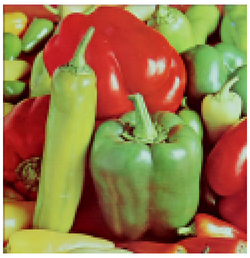

(c)

(b)

(d)

Fig. 8 Input images, and output stego-images with the watermark. (a) Image "Pepper". (b) Image "Jet". (c) and (d) Stego-images after embedding the watermark, respectively.

Table 1 PSNR values of stego-images after embedding watermarks.

	Lena	Pepper	Jet
PSNR	33.0	33.0	33.0

REFERENCES

[1] J. J. K. O'Ruanaidh and T. Pun, "Rotation, scale and translation invariant digital image watermarking," *Proceedings of IEEE International Conference on Image Processing*, Santa Barbara, CA USA, Vol. 1, pp. 536-539, Oct. 26-29, 1997.

[2] M. Wu, M. L. Miller, J. A. Bloom, and I. J. Cox, "A rotation, scale and translation resilient public watermark," *Proceedings of 1999 IEEE International Conference on Acoustics, Speech, and Signal Processing*, Phoenix, AZ, USA, Vol. 4, pp. 2065, March 15-19, 1999.

[3] C. Y. Lin, M. Wu, J. A. Bloom, I. J. Cox, M. L. Miller, and Y.M. Lui, "Rotation, scale, and translation resilient watermarking for images," *IEEE Transactions on Image Processing*, Vol. 10, Issue 5, pp. 767-782, May 2001.

[4] P. C. Su and C. C. Kuo, "An Image Watermarking Scheme to Resist Generalized Geometrical Transformations," *Proceedings of SPIE Conference on Multimedia Systems and Applications III*, Boston, Massachusetts, Vol. 4209, pp. 354-365, November 5-8, 2000.

[5] R.C. Gonzalez and R. E. Woods, "Digital Image Processing," second edition, pp. 155, 2002.

[6] http://www.ph.tn.tudelft.nl/Courses/FIP/noframes/fip-Properti-2.html, Properties of Fourier Transforms.

[7] C. Y. Lin and S. F. Chang, "Distortion Modeling and Invariant Extraction for Digital Image Print-and-Scan Process," *Proceedings of International Symposium on Multimedia Information Processing* (ISMIP), Taipei, Taiwan, Dec. 1999.

[8] A. Navarro and J. Tavares, "Joint Source-Channel PCM Image Coding for Binary Symmetric Channels," *Proceedings of International Conference on Signal Processing Applications and Technology*, Orlando, FL, USA, 1999.

[9] J. O'Ruanaidh, W. J. Dowling, and F. M. Boland, "Phase watermarking of digital images," *Proceedings of ICIP' 96*, Lausanne, Switzerland, vol. 3, pp. 239–242, Sept. 1996.